

CORROSION RESISTANCE OF Zn-Ni COATINGS EXPOSED TO NEUTRAL SALT SPRAY

**Julian Kubisztal, Jolanta Niedbala
Antoni Budniok, Eugeniusz Łągiewka**

Summary

Zn-Ni coatings (c.a. 30 wt.% Ni) have been deposited under galvanostatic conditions on a carbon steel substrate (St3S) from an ammonia bath. The corrosion resistance of the obtained coatings was examined using accelerated corrosion test (NSS – neutral salt spray) according to ISO 9227:2007. In order to compare corrosion properties of the as-deposited Zn-Ni coating, Zn-Ni coating after exposure to the NSS environment and Zn coating the potentiodynamic technique, electrochemical impedance spectroscopy (EIS) and scanning Kelvin probe (SKP) methods were used. The obtained results indicate that as-deposited and after NSS test Zn-Ni coatings exhibit better corrosion resistance in 5% NaCl than Zn coating. It was found that addition of nickel in zinc matrix improves corrosion properties of the oxide layer formed on the coating surface. Moreover Zn-Ni coating after exposure to the neutral salt spray have higher corrosion resistance in comparison with as-deposited Zn-Ni coating. It was stated that improved corrosion resistance of the Zn-Ni coatings after salt spray test could be attributed to the presence of $Zn_5(OH)_8Cl_2 \cdot H_2O$ phase formed on the coating surface.

Keywords: Zn-Ni coatings, corrosion resistance, SKP, EIS

Charakterystyka odporności korozyjnej powłok Zn-Ni poddanych działaniu obojętnej mgły solnej

Streszczenie

Elektrolityczne powłoki Zn-Ni (Ni ok. 30% mas.) wytworzono w warunkach galwanostaticznych na podłożu stalowym (S235JR) z kąpeli amoniakalnej. Powłoki Zn-Ni poddano działaniu obojętnej mgły solnej (NSS) zgodnie z ISO 9227:2007. Porównano odporność korozyjną powłok: Zn, Zn-Ni w stanie wyjściowym oraz Zn-Ni po przyspieszonych badaniach w komorze solnej. Stosowano następujące metody badań: technikę polaryzacji potencjodynamicznej, elektrochemiczną spektroskopię impedancyjną (EIS) i skaningową technikę z użyciem sondy Kelvina (SKP). Analiza wyników badań wskazuje, że powłoki Zn-Ni w stanie wyjściowym oraz poddane działaniu mgły solnej mają większą odporność korozyjną w środowisku 5% NaCl w porównaniu z powłoką Zn. Większa odporność korozyjna powłok stopowych Zn-Ni jest spowodowana przede wszystkim obecnością niklu – poprawia właściwości ochronne warstewki tlenkowej powstałej na powierzchni powłoki. Ponadto stwierdzono, że powłoki Zn-Ni w obecności mgły solnej charakteryzuje większa odporność korozyjna w porównaniu z powłokami Zn-Ni w stanie wyjściowym. Większą odporność korozyjną powłoki Zn-Ni poddanej działaniu mgły solnej można przypisać obecności produktów korozji na jej powierzchni, których głównym składnikiem jest faza $Zn_5(OH)_8Cl_2 \cdot H_2O$.

Słowa kluczowe: powłoki Zn-Ni, odporność korozyjna, SKP, EIS

Address: Prof. Antoni BUDNIOK, Prof. Eugeniusz ŁĄGIEWKA, Julian KUBISZTAL, Ph.D., Jolanta NIEDBAŁA, Ph.D., University of Silesia, Institute of Materials Science, Bankowa 12, 40-007 Katowice. Tel.+48-32-3591582, Fax: +48-32-3592133, e-mail: j.kubiszt@o2.pl (J. Kubisztal)

1. Introduction

Application of zinc alloys coatings to improve mechanical properties and corrosion resistance of steel sheets has been widely discussed [1-6]. Particularly promising are Zn-Ni coatings which can be considered as an alternative to zinc and cadmium coatings, mainly in the automotive industry. However, electrolytical production of zinc-based alloys with addition of iron group metals causes the anomalous phenomenon of co-deposition. It should be added that the alkaline plating baths are less efficient in comparison with the acidic ones but it produces more uniform and a single-phase alloy [7].

The corrosion resistance of coating depends considerably on: i) the dimension of its crystallites, ii) surface morphology, iii) presence of structural defects, iv) chemical and phase composition and v) chemical nature of the substrate. It should be emphasized that the presence of passive film placed between the coating and the environment greatly affects the corrosion resistance. Generally, a compact, adherent, insoluble and insulating (or semiconducting) passive layer serves as a good barrier against the corroding environment [7, 8].

It is known that the presence of zinc in Zn-Ni alloys provides cathodic protection of iron-based substrates while presence of nickel additionally improves protective properties of the passive oxide film [1, 3-13]. Therefore, production of Zn-Ni coatings with enhanced content of nickel is an interesting problem from both scientific and practical points of view.

The aim of this work is to investigate corrosion properties of the as-deposited and after exposure to neutral salt spray Zn-Ni coatings in 5% NaCl environment.

2. Experimental

Electrolytic Zn-Ni coatings were obtained from an alkaline plating bath having the following composition (g dm^{-3}): $\text{NiSO}_4 \cdot 7\text{H}_2\text{O}$ – 50, $\text{ZnSO}_4 \cdot 7\text{H}_2\text{O}$ – 100, Na_2SO_4 – 75, $(\text{NH}_4)_2\text{SO}_4$, – 38, NH_4OH – 250 dm^{-3} . The investigated Zn-Ni coatings have been deposited on a carbon steel substrate (S235JR, 25 cm^2) under galvanostatic conditions ($j = -30 \text{ mA cm}^{-2}$) at temperature 298 K. pH of the solution was kept in the range from 9.6 to 10.4 and the rate of stirring was 250 rpm.

Chemical composition of the Zn-Ni coatings was determined by the Energy Dispersive Spectroscopy method (EDS, Jeol JSM 6480). Qualitative phase composition of the investigated Zn-Ni coatings was determined by X-ray diffraction method (XRD) using Philips diffractometer PW 3000/60 ($\text{Cu}_{K\alpha}$ radiation) and ICDD cards.

The corrosion behaviour of Zn-Ni samples was examined using accelerated corrosion test in a fog chamber according to ISO 9227:2007. The corrosion

products formed on the investigated Zn-Ni coatings after 96 hours of exposure to the neutral salt spray were studied using XRD measurements.

In order to investigate electrochemical properties of the Zn-Ni coatings potentiodynamic technique and electrochemical impedance spectroscopy (EIS) were used. For the data registration the electrochemical system PARSTAT 2273 (potentiostat / galvanostat / FRA) and the PowerSuite software were used. The geometric surface area of all investigated electrodes was 1 cm^2 .

Electrochemical tests were performed in 5% NaCl solution using three-electrode glass cell with a platinum mesh as a counter electrode and the saturated calomel electrode (SCE) as a reference electrode.

Electrochemical measurements were performed after immersing the investigated alloy coatings in the sodium chloride solution for 20 hours. The potentiodynamic curves were recorded in the range of $\pm 150 \text{ mV}$ with respect to open circuit potential (OCP) and at scan rate 10 mV min^{-1} . The impedance measurements were performed at the corrosion potential E_{corr} in the frequency range from 10 kHz to 10 mHz. In the EIS measurements the amplitude of the *ac* signal was 10 mV. The approximation of the *a.c.* impedance spectra were performed using complex nonlinear least-square program (ZSimpWin 3.20).

Local changes of corrosion resistance of Zn-Ni coatings were investigated by scanning Kelvin probe (SKP) measurements. SKP measurements were performed on the Zn-Ni coatings using PAR Model 370 Scanning Electrochemical Workstation. The detailed description of M370 system was given in [14, 15]. The Kelvin probe was made of a tungsten wire ($\text{\O} 500 \text{ }\mu\text{m}$). The distance between the probe tip and the specimen was maintained at $100 \text{ }\mu\text{m}$.

3. Results and discussion

3.1. Characteristics of Zn-Ni coatings

It was found that in the obtained Zn-Ni coatings the content of nickel was c.a. 30 wt.%. Figure 1 shows X-ray diffraction pattern representing the phase composition of the as-deposited Zn-Ni coating. As it can be seen the X-ray spectrum consists of the lines that correspond to $\text{Ni}_2\text{Zn}_{11}$ phase.

3.2. Corrosion behavior of Zn-Ni coatings in fog chamber

Photographs of Zn-Ni coatings before and after NSS test were shown in Fig 2. The first marks of white rust (Zn oxide) on the Zn-Ni coating surface were detected after c.a. 7 h of exposure. It should be added that after 96 hours of exposure to the NSS environment the corrosion of carbon steel substrate was not observed. Fig. 3 shows the phase composition of corrosion products. It was found that $\text{Zn}_5(\text{OH})_8\text{Cl}_2 \cdot \text{H}_2\text{O}$ is the main corrosion product that is formed on the Zn-Ni coating surface under accelerated corrosion conditions in the fog chamber. According to [16] immersion of zinc and zinc alloys in neutral solution

causes that an oxide and/or hydroxide layer is formed spontaneously. Such film forms the basis for a growth of the corrosion products. When additionally chloride ions are present on the coating surface, zinc hydrochlorides with a different number of water molecules may be formed [7].

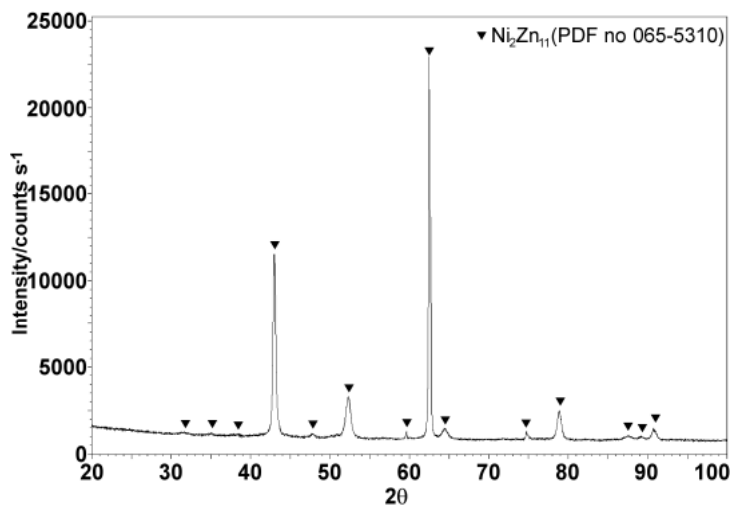


Fig. 1. X-ray diffraction pattern of the as-deposited Zn-Ni coating

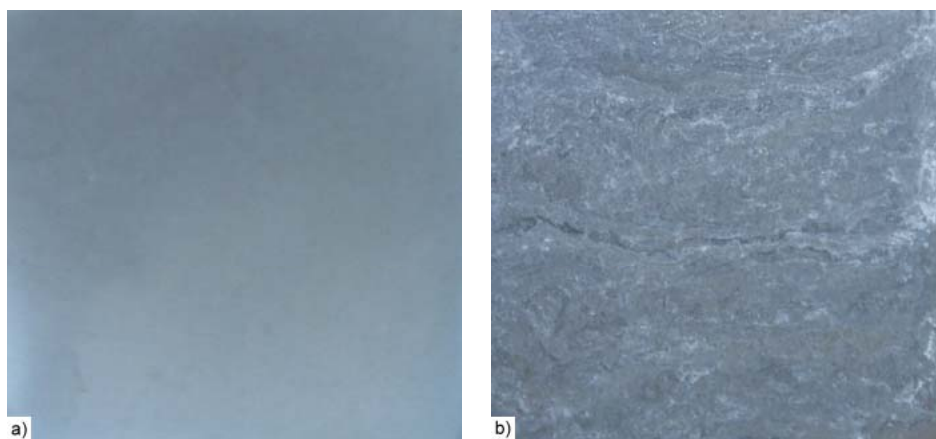


Fig. 2. Photographs of the as-deposited (a) and after NSS test (b) Zn-Ni coating

SKP technique is a non-destructive electrochemical scanning method allowing measurements of contact potential difference V_{CPD} distribution over the surface of the coating [17-20]. In principle the Kelvin probe measures the work

function of a sample using the vibrating condenser method. The current induced by the vibration is compensated by external voltage and thus at zero current the external voltage is equal to the contact potential difference. It should be added that using Kelvin probe it can be measured the surface topography, as well.

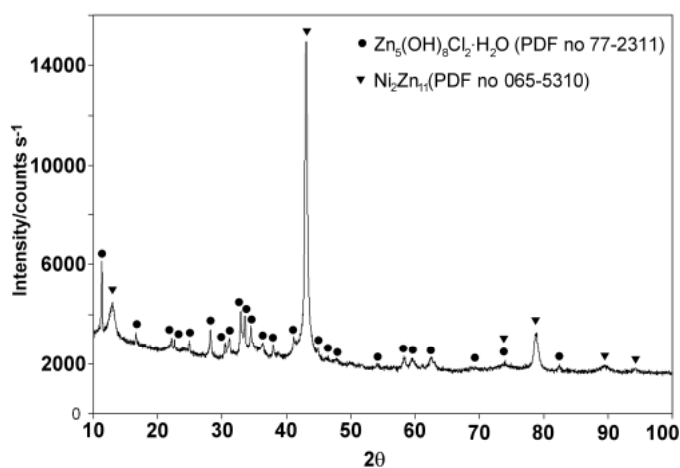


Fig. 3. X-ray diffraction patterns of the Zn-Ni coating after NSS test

Contact potential difference V_{CPD} distribution measured over the examined coatings are presented in Figs. 4 a, b, c. The contact potentials obtained for Zn-Ni coating after NSS test and for as-deposited Zn-Ni coating exhibit a shift (c.a. 350 mV and c.a. 50 mV, respectively) to the more negative values in comparison with zinc coating. It should be noted that values of V_{CPD} are proportional to the difference of work functions determined for coating | passive layer | Kelvin probe system. Thus for as-deposited and after NSS test Zn-Ni coatings it is more difficult to remove an electron from their surface. It means that flow of electric charge is impeded. Such behavior suggests that addition of nickel in zinc-based alloys coatings improves protective properties of passive layer in comparison with bare zinc coating. Moreover, determined values of V_{CPD} indicate that the presence of corrosion products formed on the Zn-Ni coating after NSS test additionally improves its corrosion properties.

The surface topography of the examined coatings are presented in Figs. 5 a, b, c. As it can be noticed in these figures, the presence of the nickel in zinc matrix causes a decrease of the surface porosity of the alloy in relation to zinc coating. Moreover, it can be stated, that the Zn-Ni coating exposed to the neutral salt spray environment are characterized by more porous surface with respect to as-deposited Zn-Ni coating.

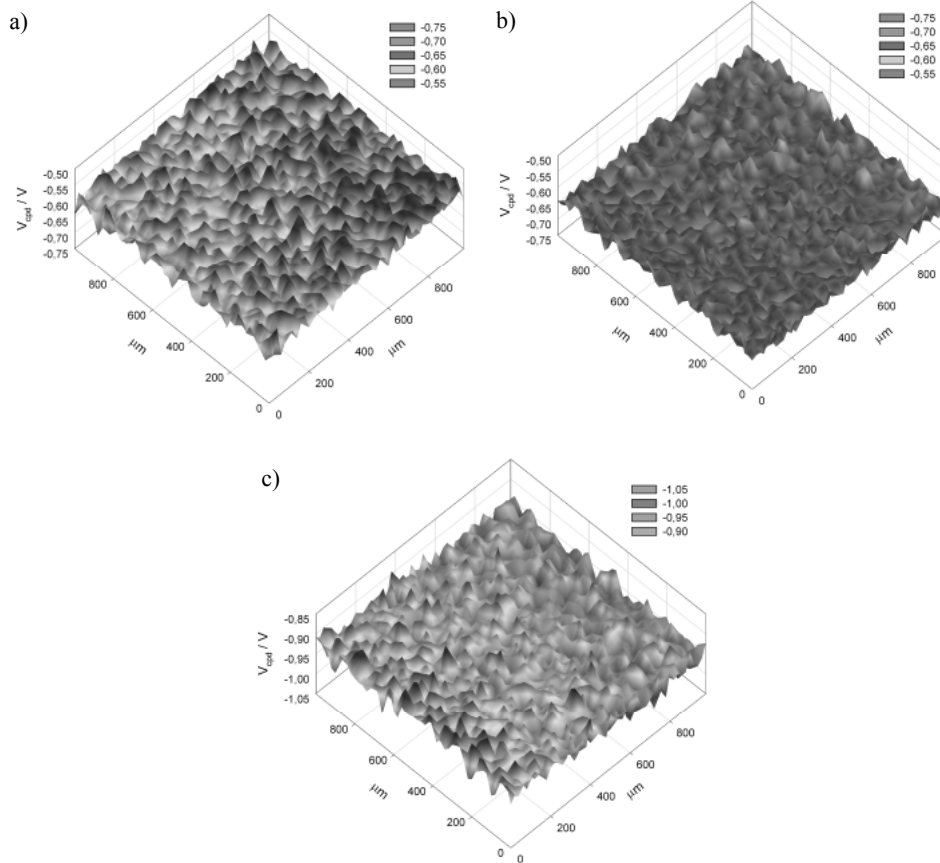


Fig. 4. Contact potential difference V_{CPD} distribution measured on Zn coating (a), as-deposited Zn-Ni coating (b) and after NSS test Zn-Ni coating (c).

3.3. Corrosion resistance of Zn-Ni coatings in a 5% NaCl solution

In Figure 6 the polarization curves determined for Zn-Ni coatings before and after NSS test were compared to the curve obtained for zinc coating. As it was shown in Fig. 6 the obtained polarization curves consist of two Tafel segments corresponding to cathodic and anodic partial reactions. Corrosion parameters, i.e. corrosion potential E_{corr} and corrosion current density j_{corr} were determined using Butler-Volmer equation [21, 22]. The obtained results are gathered in Tab. 1.

The corrosion potential obtained for Zn-Ni coating after NSS test exhibits a shift to the right-hand side in comparison with as-deposited coating. Moreover, in comparison with as-deposited Zn-Ni coating the decrease of corrosion current

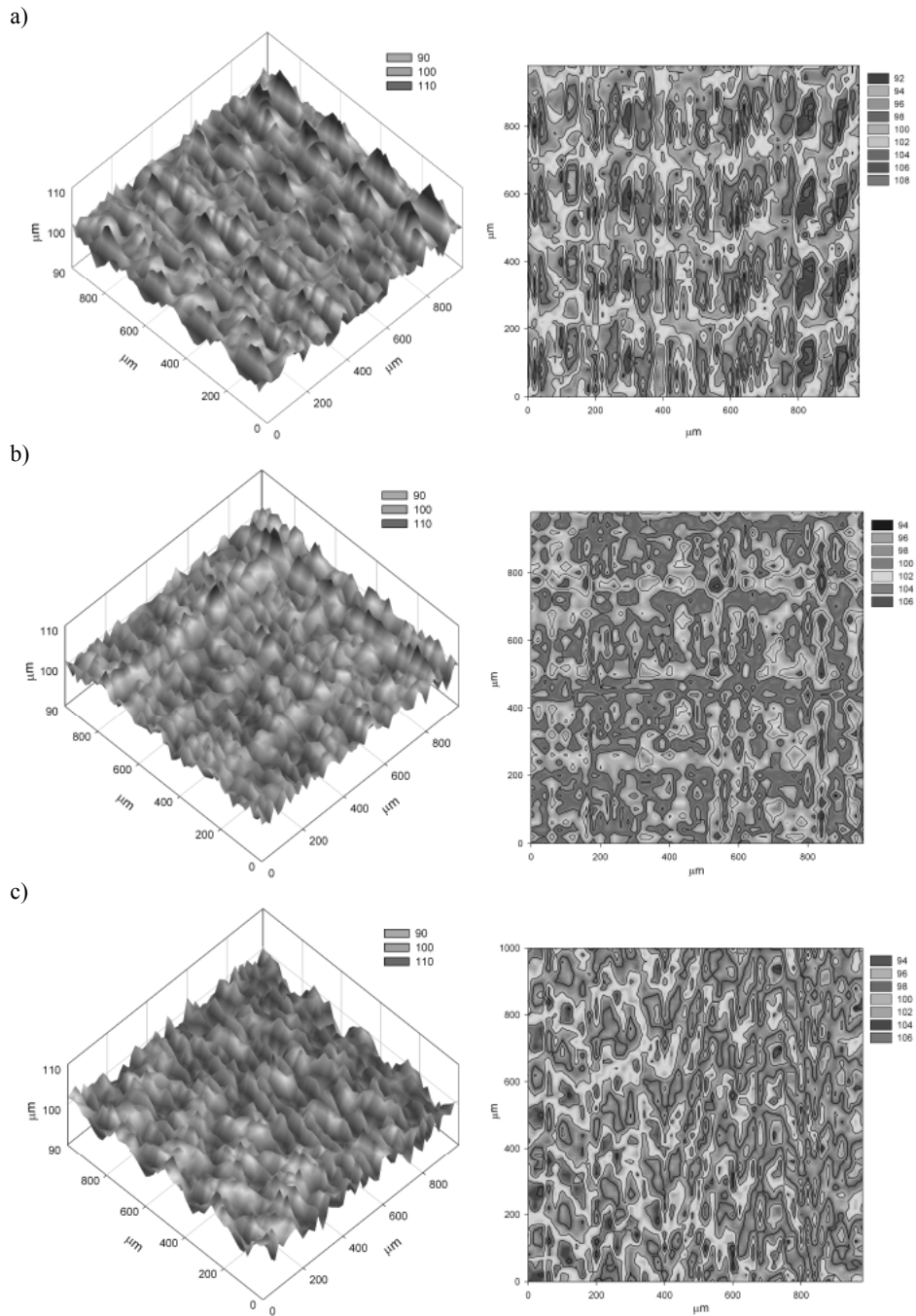


Fig. 5. Surface topography (2D and 3D) of the Zn coating (a), as-deposited Zn-Ni coating (b) and after NSS test Zn-Ni coating (c)

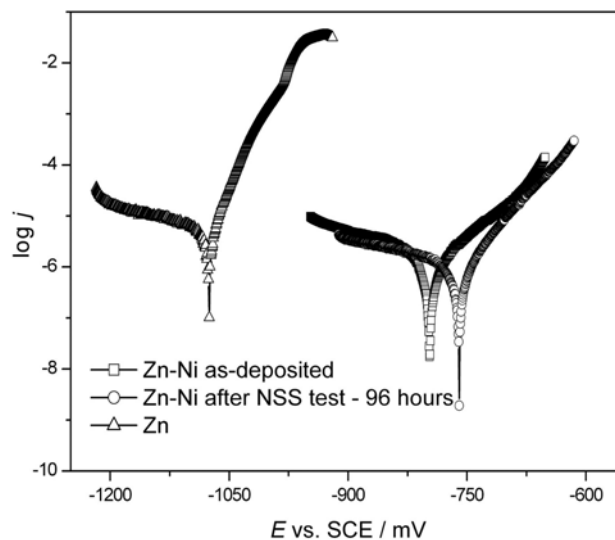


Fig. 6. Polarization curves obtained for Zn coating, as-deposited Zn-Ni coating and Zn-Ni coating after NSS test in 5% NaCl solution

Table 1. The corrosion parameters of the Zn-Ni coatings, measured in 5% NaCl solution

Coatings	Corrosion parameters		
	$E_{\text{corr}} / \text{mV}$	$j_{\text{corr}} / \mu\text{A cm}^{-2}$	$R_p / \text{k}\Omega \text{ cm}^2$
Zn-Ni (as-deposited)	-796	3.1	11.5
Zn-Ni (after NSS test)	-760	1.3	18.4
Zn	-1075	6.0	1.1

density was observed (c.a. 2.4 times). It should be also noted that the polarization resistance (calculated from the Stern-Geary equation [23]) of the Zn-Ni coating after NSS test is c.a. 7 k Ω higher than that of the as-deposited coating. All discussed above parameters indicate on improved corrosion resistance of the Zn-Ni coatings after salt spray test in comparison with as-deposited coating. This behavior could be attributed to the additional phase ($\text{Zn}_5(\text{OH})_8\text{Cl}_2 \cdot \text{H}_2\text{O}$) formed on the coating surface [7]. It should be added that corrosion parameters determined for zinc coating clearly suggest that the as-deposited and after NSS test zinc-based alloy with addition of nickel exhibit better corrosion resistance.

Fig. 7 shows the complex plane plots $-Z''(\omega)$ versus $Z'(\omega)$ (where ω is the angular frequency, $Z'(\omega)$ and $Z''(\omega)$ are the real and imaginary part of the

measured impedance, respectively) for as-deposited, after NSS test Zn-Ni coatings and zinc coating.

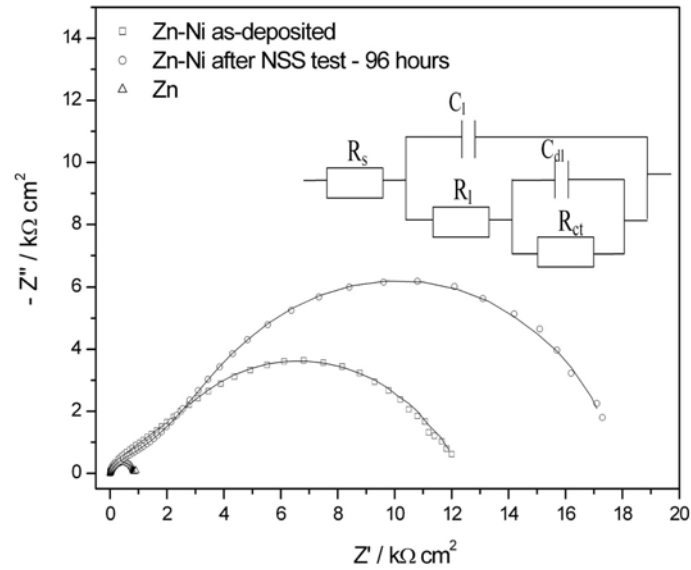


Fig. 7. Complex plane plots obtained for Zn coating, as-deposited Zn-Ni coating and Zn-Ni coating after NSS test in 5% NaCl solution. Symbols are the experimental data and lines were modeled using the EEC model (inset)

Nyquist plots reveal two relaxation processes in high- and low- frequency range. It is known that oxide layer capacitances are generally very low and the impedance response of oxide layers is usually located in the high frequency region [16].

For approximation of the impedance data a ladder model was used (Fig. 7 – inset). This electrical equivalent circuit (EEC) predicts two time constants. In particular high-frequency time constant could be attributed to the formation of the porous oxide layer (corrosion products) and the low-frequency time constant to the activation process which is characterized by charge transfer resistance R_{ct} and double layer capacitance C_{dl} . As a result of approximation one can obtain five parameters which were gathered in Tab. 2. It should be added that in this model the capacitances C_l , C_{dl} were replaced by a constant phase element ($Z_{CPE} = 1/T(j\omega)^\phi$) where empirical exponent ϕ takes into account a distribution of time constant which may result from inhomogeneities and/or discontinuity of the coating surface caused for example by the presence of the corrosion products [16, 24-27]. Parameter T is associated with the double layer capacitance by relation: $C_{dl} = T(\omega^*)^{\phi-1}$ where $\omega^* = (R_{ct}T)^{-1/\phi}$ [28].

Table 2. Equivalent circuit parameters determined by modeling of the impedance spectra

Parameters	Zn-Ni as-deposited	Zn-Ni after NSS test	Zn
Solution resistance R_s , $\Omega \text{ cm}^2$	2.77±0.15	1.89±0.43	1.96±0.07
Empirical exponent ϕ_1	0.859±0.006	0.743±0.007	0.92±0.08
Capacitance of oxide layer C_1 , $\mu\text{F cm}^{-2}$	0.99	0.94	16.10
Resistance of oxide layer R_1 , $\text{k}\Omega \text{ cm}^2$	1.28±0.08	1.58±0.08	0.006±0.002
Empirical exponent ϕ_{dl}	0.651±0.015	0.710±0.014	0.806±0.012
Double layer capacitance C_{dl} , $\mu\text{F cm}^{-2}$	14.70	25.88	115.30
Charge transfer resistance R_{ct} , $\text{k}\Omega \text{ cm}^2$	11.31±0.23	17.56±0.38	0.88±0.02

For the as-deposited and after NSS test Ni-Zn coatings, the exponents ϕ_1 and ϕ_{dl} (i.e. empirical exponents obtained by replacing C_1 and C_{dl} with CPE elements) change from 0.92 to 0.65 what indicates that the CPE components behave like capacitive reactances. Notice that, in the low-frequency range, for both as-deposited and after NSS test coatings the exponent ϕ_{dl} is in the range 0.65-0.71 what indicates that the value of C_{dl} is strongly dispersed probably due to formation of porous oxide layer.

The values of the R_{ct} obtained for the Zn-Ni after NSS test coating are c.a. 6.3 $\text{k}\Omega$ higher in comparison with as-deposited coating suggesting their better corrosion resistance. Moreover, the resistance R_1 determined for as-deposited and after NSS test Zn-Ni coatings is comparable. It should be added that R_1 is c.a. 9 and 11 times lower than R_{ct} for as-deposited and after NSS test Zn-Ni coatings, respectively. Such low R_1 values could be attributed to fast local corrosion processes i.e. in neutral solution zinc hydroxide is converted into oxide (formation of oxide layer) [16]. Notice that the double layer capacitance for as-deposited Zn-Ni coating is c.a. 7.8 times lower and for Zn-Ni coating after NSS test 4.5 times lower in comparison with zinc coating. This behavior may be attributed to the decrease in the real surface area [29] of Zn-Ni coatings.

The oxide layer formed on Zn-Ni coatings is thicker (the reciprocal of C_1 is directly proportional to layer thickness [26]) and of higher resistance in comparison with the zinc coating. Thus it should be stated that the better corrosion resistance of Zn-Ni coating results from the improved corrosion properties of the oxide layer probably caused by the presence of the nickel in zinc matrix.

4. Concluding remarks

It was found that as-deposited and after neutral salt spray test Zn-Ni coatings exhibit better corrosion resistance in 5% NaCl than Zn coating. Higher

corrosion resistance of Zn-Ni coatings results from improved protective properties of the corrosion products layer what is caused by addition of nickel in zinc matrix. It was stated that corrosion resistance of the Zn-Ni coating after salt spray test is higher in comparison with the as-deposited Zn-Ni coating what could be attributed to the presence of $Zn_5(OH)_8Cl_2 \cdot H_2O$ phase formed on the coating surface.

Acknowledgements

This work was financially supported by PBZ-MNiSW-4/01/1/2007.

References

- [1] M.E. SOARES, C.A.C. SOUZA, S.E. KURI: Corrosion resistance of a Zn-Ni electrodeposited alloy obtained with a controlled electrolyte flow and gelatin additive. *Surf. Coat. Technol.*, **201**(2006)6, 2953-2959.
- [2] H. ASHASSI-SORKHABI, A. HAGRAH, N. PARVINI-AHMADI, J. MAN-ZOORI: Zinc-nickel alloy coatings electrodeposited from a chloride bath using direct and pulse current. *Surf. Coat. Technol.*, **140**(2001)3, 278-283.
- [3] C.C. LIN, C.M. HUANG: Zinc-Nickel alloy coatings electrodeposited by pulse current and their corrosion behavior. *J. Coat. Technol. Research*, **3**(2006)2, 99-104.
- [4] A.P. ORDINE, S.L. DIAZ, I.C.P. MARGARIT, O.R. MATTOS: Zn-Ni and Zn-Fe alloy deposits modified by P incorporation: anticorrosion properties. *Electrochim. Acta.*, **49**(2004)17-18, 2815-2823.
- [5] N. PISTOFIDIS et al.: The combined effect of nickel and bismuth on the structure of hot-dip zinc coatings. *Mat. Let.*, **61**(2007)10, 2007-2010.
- [6] R. FRATESI et al.: Contemporary use of Ni and Bi in hot-dip galvanizing. *Surf. Coat. Technol.*, **157**(2002)1, 34-39.
- [7] O. GIRČIENĖ et al.: Corrosion resistance of phosphated Zn-Ni alloy electrodeposits. *Surf. Coat. Technol.*, **203**(2009)20-21, 3072-3077.
- [8] X. Zhang et al.: Characterization of chromate conversion coatings on zinc using XPS and SKPFM. *Surf. Coat. Technol.*, **197**(2005)2-3, 168-176.
- [9] R. Ramanauskas et al.: Pulse plating effect on microstructure and corrosion properties of Zn-Ni alloy coatings. *J. Solid State Electrochem.*, **9**(2005)12, 900-908.
- [10] B. VEERARAGHAVAN, H. KIM, B. POPOV: Optimization of electroless Ni-Zn-P deposition process: experimental study and mathematical modeling. *Electrochim. Acta*, **49**(2004)19, 3143-3154.
- [11] C.E. LEHMBERG, D.B. LEWIS, G.W. MARSHALL: Composition and structure of thin electrodeposited zinc-nickel coatings. *Surf. Coat. Technol.*, **192**(2005)2-3, 269-277.
- [12] I. BROOKS, U. ERB: Hardness of electrodeposited microcrystalline and nanocrystalline γ -phase Zn-Ni alloys. *Scripta Materialia*, **44**(2001)5, 853-858.
- [13] J. FEI, G.D. WILCOX: Electrodeposition of zinc-nickel compositionally modulated multilayer coatings and their corrosion behaviours. *Surf. Coat. Technol.*, **200**(2006)11, 3533-3539.

- [14] I. ANNERGREN, F. ZOU, D. THIERRY: Application of localised electrochemical techniques to study kinetics of initiation and propagation during pit growth. *Electrochim. Acta*, **44**(1999)24, 4383-4393.
- [15] G. BARIL et al.: Local electrochemical impedance spectroscopy applied to the corrosion behavior of an AZ91 magnesium alloy. *J. Electrochem. Soc.*, **150**(2003)10, B488-B493.
- [16] N. IBRIŞ et al.: Comparative EIS study of a paste electrode containing zinc powder in neutral and near neutral solutions. *J. Solid State Electrochem.*, **6** (2002)2, 119-125.
- [17] A.Q. FU, Y.F. CHENG: Characterization of corrosion of X65 pipeline steel under disbonded coating by scanning Kelvin probe. *Corrosion Science*, **51**(2009)4, 914-920.
- [18] A. TAHARA, T. KODAMA: Potential distribution measurement in galvanic corrosion of Zn/Fe couple by means of Kelvin probe. *Corrosion Science*, **42**(2000)4, 655-673.
- [19] C.K. CHUNG, W.T. CHANG, R.X. ZHOU: Effect of cobalt content on the work function of the electrodeposited nickel-cobalt films. *Microsyst. Technol.*, **14**(2008)9-11, 1389-1394.
- [20] K. WAPNER, M. STRATMANN, G. GRUNDMEIER: Application of the scanning Kelvin probe for the study of the corrosion resistance of interfacial thin organosilane films at adhesive/metal interfaces. *Silicon Chemistry*, **2**(2005)5-6, 235-245.
- [21] J. O'M. BOCKRIS, A.K.N. REDDY: Modern Electrochemistry, vol. 2, Plenum Press, New York 1977, 883.
- [22] E. MCCAFFERTY: Validation of corrosion rates measured by the Tafel extrapolation method. *Corrosion Science*, **47**(2005)12, 3202-3215.
- [23] M. STERN, A.L. GEARY: Electrochemical polarization: I. A theoretical analysis of the shape of polarization curves. *J. Electrochem. Soc.*, **104**(1957)1, 56-63.
- [24] M.C. LI et al.: Electrochemical corrosion behavior of nanocrystalline zinc coatings in 3.5% NaCl solutions. *J. Solid State Electrochem.*, **11**(2007)9, 1319-1325.
- [25] Y. HAMLAOUI, F. PEDRAZA-DIAZ, L. TIFOUTI: Comparative Study by EIS on the corrosion resistance of electroplated Zn coating in different corrosive media. *J. Eng. App. Sci.*, **2**(2007)4, 706-713.
- [26] K.M. ISMAIL: Electrochemical behaviour of cadmium in NaOH solution. *J. App. Electrochem.*, **31**(2001)12, 1333-1338.
- [27] B. SZCZYGIEL, M. KOŁODZIEJ: Composite Ni/Al₂O₃ coatings and their corrosion resistance. *Electrochim. Acta*, **50**(2005)20, 4188-4195.
- [28] C.H. HSU, F. MANSFELD: Technical Note: Concerning the conversion of the constant phase element parameter Y₀ into a capacitance. *Corrosion*, **57**(2001)9, 747-748.
- [29] M. BOUNOUGHAZ et al.: A comparative study of the electrochemical behaviour of Algerian zinc and a zinc from a commercial sacrificial anode. *J. Mat. Sci.*, **38**(2003)6, 1139-1145.

Received in January 2010